

PNE-238F

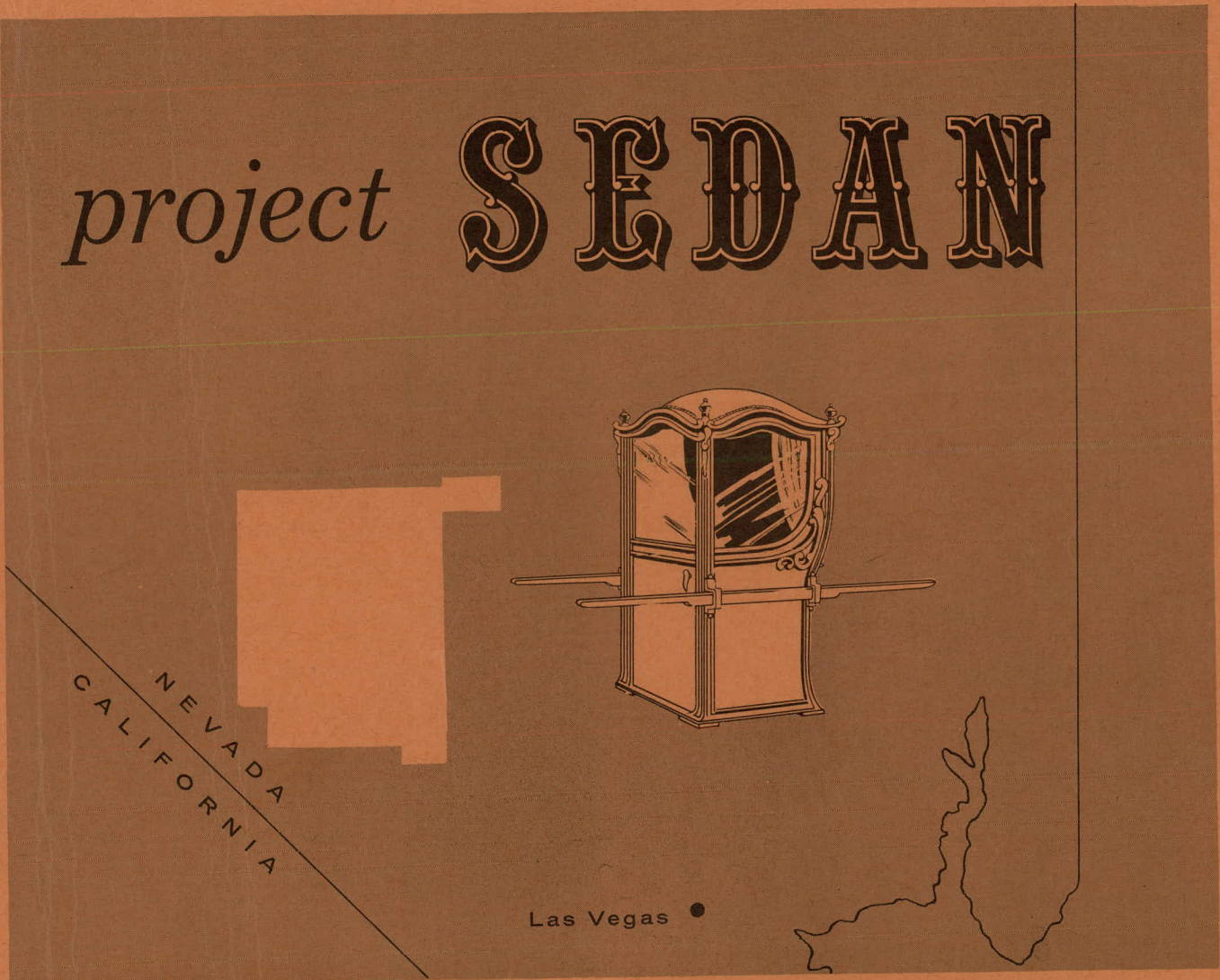
FINAL REPORT

MASTER


Plowshare / peaceful uses for nuclear explosives

UNITED STATES ATOMIC ENERGY COMMISSION / PLOWSHARE PROGRAM

project **SEDAN**



**Interception and Retention of Radioactive Fallout
by Desert Shrubs in the Sedan Fallout Field**

William E. Martin

UCLA SCHOOL OF MEDICINE

ISSUED: DECEMBER 10, 1965

DISCLAIMER

This report was prepared as an account of work sponsored by an agency of the United States Government. Neither the United States Government nor any agency Thereof, nor any of their employees, makes any warranty, express or implied, or assumes any legal liability or responsibility for the accuracy, completeness, or usefulness of any information, apparatus, product, or process disclosed, or represents that its use would not infringe privately owned rights. Reference herein to any specific commercial product, process, or service by trade name, trademark, manufacturer, or otherwise does not necessarily constitute or imply its endorsement, recommendation, or favoring by the United States Government or any agency thereof. The views and opinions of authors expressed herein do not necessarily state or reflect those of the United States Government or any agency thereof.

DISCLAIMER

Portions of this document may be illegible in electronic image products. Images are produced from the best available original document.

LEGAL NOTICE

This report was prepared as an account of Government sponsored work. Neither the United States, nor the Commission, nor any person acting on behalf of the Commission:

A. Makes any warranty or representation, expressed or implied, with respect to the accuracy, completeness, or usefulness of the information contained in this report, or that the use of any information, apparatus, method, or process disclosed in this report may not infringe privately owned rights; or

B. Assumes any liabilities with respect to the use of, or for damages resulting from the use of any information, apparatus, method, or process disclosed in this report.

As used in the above, "person acting on behalf of the Commission" includes any employee or contractor of the Commission, or employee of such contractor, to the extent that such employee or contractor of the Commission, or employee of such contractor prepares, disseminates, or provides access to, any information pursuant to his employment or contract with the Commission, or his employment with such contractor.

This report has been reproduced directly from the best available copy.

Printed in USA. Price \$2.00. Available from the Clearinghouse for Federal Scientific and Technical Information, National Bureau of Standards, U. S. Department of Commerce, Springfield, Virginia 22151.

PROJECT SEDAN

PROJECT 62.83

INTERCEPTION AND RETENTION OF RADIOACTIVE FALLOUT
BY DESERT SHRUBS IN THE SEDAN FALLOUT FIELD

William E. Martin, Ph. D.

Laboratory of Nuclear Medicine
and Radiation Biology

University of California
Los Angeles, California

ABSTRACT

- (1) Concentrations of I^{131} and Sr^{89} on plants contaminated by fallout from Project Sedan tended to decrease with increasing distance from ground zero and increasing time after the detonation. (2) Microscopic and radiometric examinations of foliage indicated that most of the activity deposited on leaves was probably due to particles $< 5 \mu$ in diameter, and virtually none of it was due to particles $> 44 \mu$ in diameter. (3) A comparison between the theoretical and observed interrelations of gamma dose rates, ~~I^{131} and Sr^{89}~~ deposition rates, and ~~I^{131} and Sr^{89}~~ interception by desert shrubs indicated a deficiency of I^{131} relative to Sr^{89} in areas more than 40 mi. from ground zero and an excess of both I^{131} and Sr^{89} relative to dose rates in areas about 100 mi. from ground zero. (4) The effective half-lives of I^{131} and Sr^{89} on plants were shorter than their radioactive half-lives, and a comparison of environmental half-lives suggested that I^{131} may have been lost from plants by some process, such as vaporization, which had no effect on the retention of Sr^{89} . (5) Statistical analyses indicated that the frequency distributions of variates representing maximum concentrations of ~~I^{131} and Sr^{89}~~ on plants, and in the tissues of rabbits collected at the same times and locations in the fallout field, were not normal but lognormal. Similar analyses indicated that the frequency distributions of effective half-life estimates could be treated as either normal or lognormal. 16 references. send.

These studies were supported by Contract AT(04-1)GEN-12 between the U. S. Atomic Energy Commission and the University of California.

CONTENTS

ABSTRACT	2
1.0 INTRODUCTION.	4
1.1 Background.	4
1.2 Objectives	5
1.3 Literature	6
2.0 METHODS.	6
2.1 Collection and Radiochemical Analyses of Samples	6
2.2 Analyses of Foliage Samples	8
2.3 Calculation of Retention Factors.	8
2.4 Calculation of Interception Factors.	9
2.5 Statistical Analyses of Frequency Distributions.	11
3.0 RESULTS.	12
3.1 Radionuclide Concentrations in Plant Samples & Rabbit Tissues.	12
3.2 Fallout Particles and Radioactivity on Plant Foliage	14
3.3 Retention Factors: Effective & Environmental Half-lives.	17
3.4 Interception Factors: Deposition on Soil vs. Interception by Plants.	19
3.5 Frequency Distribution of Variates	21
4.0 DISCUSSION.	29
4.1 Radionuclide Concentrations in Plant Samples & Rabbit Tissues.	29
4.2 Fallout Particles and Radioactivity on Plant Foliage	29
4.3 Retention Factors: Effective & Environmental Half-lives	30
4.4 Interception Factors: Deposition on Soil vs. Interception by Plants.	31
4.5 Lognormal vs. Normal Frequency Distributions	33
REFERENCES CITED	36
APPENDIX A	38
APPENDIX B.	39

INTERCEPTION AND RETENTION OF RADIOACTIVE FALLOUT

BY DESERT SHRUBS IN THE SEDAN FALLOUT FIELD

1.0 INTRODUCTION

1.1 Background.

The interception and retention of fallout particles by plants is rapidly followed by the appearance of radionuclides in terrestrial food chains involving a variety of plants and animals including man. The amounts of radionuclides available for ingestion and assimilation by herbivores depend, to a large extent, upon the amounts intercepted and retained by plants. The rates at which different radionuclides may be ingested by herbivores and subsequently transferred to higher trophic levels depend, to some extent, upon the rates of loss from fallout-contaminated plants. A better understanding of these interrelations should lead to a better evaluation of the biological hazards involved in the applications of nuclear energy which routinely or accidentally result in the release of radionuclides to the environment.

The initial distribution of radionuclides in a close-in fallout field is theoretically related to the gross gamma dose rate pattern at some reference time after the detonation. One might expect to find a similar relationship between dose rates and the initial distribution of radionuclides on fallout-contaminated plants; but this relationship could be confounded by fractionation, by variations in the particle-size composition of fallout, and/or by variations in the morphological characteristics of different plant species. The time-specific relationship between radionuclide concentrations on plants and in the tissues of herbivores may be further complicated by variations in the rates of loss from plants and in the rates of ingestion,

assimilation, and elimination by the herbivores.

The interpretation and evaluation of data related to gamma dose rates and to radionuclide concentrations in fallout, on plants, and in animal tissues are made difficult by their extreme range and variability. Many of the variates encountered do not have normal frequency distributions; and the use of ordinary statistical methods, which are based on the normal frequency distribution, may lead to erroneous conclusions. In this paper, I hope to provide evidence that some (perhaps most) of these variates have lognormal frequency distributions; and this obviates a real need for the development or adaptation of statistical methods to be used in the analysis of lognormal distributions.

1.2 Objectives.

In relation to some of the problems mentioned above, the objectives of this paper are to provide data concerning: (a) the concentrations of I^{131} and Sr^{89} in plants and rabbits collected between 5 and 60 days after the detonation from different parts of the Sedan fallout field, (b) the particle-size composition and gamma activity of fallout intercepted by the foliage of desert shrubs, (c) the variability of fallout retention as shown by estimates of the effective and environmental half-lives of I^{131} and Sr^{89} on fallout-contaminated plants, (d) the theoretical and observed interrelations of H + 24 gamma dose rates, fallout deposition, interception, and the initial concentrations of I^{131} and Sr^{89} on plants, and (e) the probability that the frequency distributions of variates representing the effective half-lives of I^{131} and Sr^{89} on plants, the maximum concentrations of I^{131} and Sr^{89} on plants, and the maximum concentrations of I^{131} and Sr^{89} in the thyroids and bone ash of rabbits collected at the same times and places are lognormal rather than normal.

1.3 Literature.

It is not within the scope of this paper to review the literature concerning the interception and retention of fallout by plants. A brief review and list of references on this subject were given by Martin ⁽¹⁾, and additional references have been cited by Romney et al. ⁽²⁾ and the National Academy of Science ⁽³⁾. The uses and potential uses of radiometric and radiochemical data in formulating deterministic and stochastic models to represent the time-specific relationship between radionuclide concentrations on plants and in animal tissues have been discussed by Turner ⁽⁴⁾, Turner and Martin ^(5,6), Martin ⁽⁷⁾, and Martin and Turner ⁽⁸⁾. (N. B. The papers just cited include additional lists of references.)

2.0 METHODS

2.1 Collection and Radiochemical Analyses of Samples.

Project Sedan involved the explosion of a 100 ± 15 kiloton thermonuclear bomb at a depth of 635 ft. in alluvium at the north end of the Nevada Test Site ⁽⁹⁾. The local fallout pattern resulting from this detonation and the approximate locations at which plant samples and rabbits were collected before and after the detonation are shown in Fig. 1.

Bulk plant samples and rabbit tissue samples were analyzed to determine their I^{131} and Sr^{89} contents at times of collection ranging from 5 to 60 days after the detonation on July 6, 1962. The methods used in collecting, processing, and analyzing these samples have been described in previous reports ^(5,8).

Analyses were also made to determine the time of collection concentrations of Sr^{90} and Cs^{137} in plant samples, but these data (Appendix A) have not been used in the present study because postshot concentrations at more

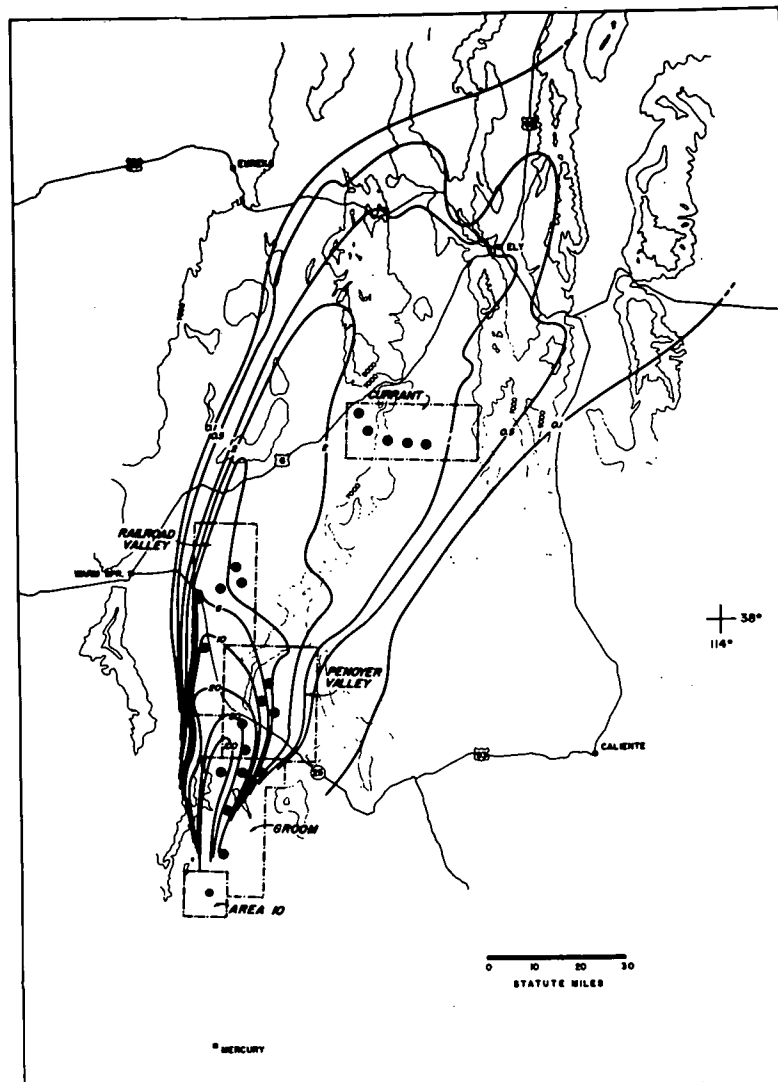


Figure 1. The Sedan fallout pattern: The black dot in Area 10 shows the approximate location of ground zero. The other black dots show the approximate locations at which plants and animals were collected after the detonation. The dose rate contours (mr/hr, 3 ft. above ground, 24 hr. after the detonation) were based on aerial survey data⁽¹⁰⁾.

than half of the 20 stations shown in Fig. 1 were not significantly higher than preshot background concentrations.

2.2. Analyses of Foliage Samples.

Foliage samples were collected to determine the number and size of radioactive particles per unit area of leaf surface. The leaves used for this purpose were first fixed on transparent sheets of gummed paper and then covered with blotting paper to hold them firmly in place. Within a day or two after collection, gross gamma counts (c/m) were obtained for each sheet. These counts were used to determine exposure times for X-ray films which were placed in contact with the gummed paper to make autoradiographs. The autoradiographs were used as maps to locate radioactive particles which were then examined microscopically and measured with an ocular micrometer. After measuring leaf surface areas (one side only) with a planimeter, the results were expressed as numbers of particles $< 20 \mu$, $20-44 \mu$, and $> 44 \mu$ diameter per square centimeter (p/cm^2). (N. B. Since the optical resolution of the lens system used in making most of these measurements is between 5 and 7μ , particles $< 5 \mu$ in diameter were not observed.) Gross gamma counts were corrected for geometry (based on a Cs^{137} standard) and for radioactive decay ($t^{-1.2}$). The results were expressed as counts per minute per square centimeter ($c/m/cm^2$) at the times of collection.

2.3 Calculation of Retention Factors.

Retention factors were estimated in terms of the effective half-lives of I^{131} and Sr^{89} on fallout-contaminated plants. The calculations were based on equations 1-3.

$$T_p = 0.693 (t_2 - t_1) / \log_e (P_{t_1} / P_{t_2}) \quad (1)$$

where, T_p = effective half-life in days

t_1 = five days after the detonation

t_2 = more than five days after the detonation

P_{t_1} = pc/g (dry wt) at t_1

P_{t_2} = pc/g (dry wt) at t_2

Estimates of environmental half-lives (i. e., the rates of loss due to factors other than radioactive decay) were based on

$$T_E = T_r \times T_p / T_r - T_p \quad (2)$$

where, T_E = environmental half-life in days (variable)

T_r = radioactive half-life in days (8.04 d I^{131} , 50.5 d Sr^{89})

T_p = effective half-life in days (variable)

Values obtained for $T_E(Sr^{89})$ were usually larger than those obtained for $T_E(I^{131})$. To estimate the difference (T_d) in half-life terms, calculations were based on

$$T_{dsi} = T_{Es} \times T_{Ei} / T_{Es} - T_{Ei} \quad (3)$$

where, T_{dsi} = a half-life term representing the difference between $T_E(I^{131})$ and $T_E(Sr^{89})$

T_{Es} = environmental half-life of $Sr^{89} = T_E(Sr^{89})$

T_{Ei} = environmental half-life of $I^{131} = T_E(I^{131})$

2.4 Calculation of Interception Factors.

Comparisons between the hypothetical and observed interrelations of gamma dose rates, fallout deposition, and the interception of I^{131} and Sr^{89} by plants were based on equations 4-7.

$$a_s = F Y \lambda_r / D C R \quad (4)$$

$$a_p = P_o / R_o \quad (5)$$

$$P_o = P_t e^{\lambda_p t} \quad (6)$$

$$f_p = a_p G / a_s \quad (7)$$

Where, a_s = theoretical deposition rate on bare soil (pc/ft²/mr/hr)

$$F = 1.43 \times 10^{23} \text{ fissions of } U^{235} / \text{kiloton yield} \quad (11)$$

$$Y_1 = 3.10 \times 10^{-2} \text{ atoms of } I^{131} / \text{fission of } U^{235} \quad (12)$$

$$Y_2 = 4.79 \times 10^{-2} \text{ atoms of } Sr^{89} / \text{fission of } U^{235} \quad (12)$$

$$\lambda_{r1} = 8.64 \times 10^{-2} \text{ dis/atom of } I^{131} / \text{day} = 0.693/8.04$$

$$\lambda_{r2} = 1.37 \times 10^{-2} \text{ dis/atom of } Sr^{89} / \text{day} = 0.693/50.5$$

$$D = 3.20 \times 10^3 \text{ dis/pc/day}$$

$$C = 2.79 \times 10^7 \text{ ft}^2/\text{mi}^2$$

$$R = 4.50 \times 10^4 \text{ mr/hr/kt/mi}^2, \text{ 24 hr. after the detonation} \quad (13)$$

a_p = observed deposition rate on plants (pc/g/mr/hr)

P_o = initial concentration (pc/g) on plants (N. B. This is a hypothetical value based on extrapolation to the time of detonation.)

R_o = mr/hr, 3 ft. above ground, 24 hr. after the detonation

P_t = pc/g (dry wt.) at the time of collection

λ_p = effective decay constant on plants = $0.693 / T_p$

f_p = fraction of I^{131} or Sr^{89} intercepted by plants (N. B.

Percentage interception = $100 f_p$.)

G = dry wt. density of plants in g/ft²

Percentage interception estimates ($100 f_p$) were based on an assumed value of $G = 20 \text{ g/ft}^2$. Estimates of a_p were based on estimates of P_o and R_o at 5 stations in each of the study areas shown in Fig. 1. The P_o estimates used for this purpose were all based on samples collected 5 days after the detonation.

2.5 Statistical Analyses of Frequency Distributions.

A preliminary study of the I^{131} data (6) indicated that the frequency distributions of variates representing I^{131} concentrations in plant samples and in the thyroids of rabbits were not normal but lognormal. Simulated samples of P_o (maximum possible concentrations of I^{131} and Sr^{89} on plants) and of A_m (maximum observed concentrations of I^{131} in the thyroids and of Sr^{89} in the bone ash of rabbits) were obtained by extrapolating the concentrations observed at different times of collection to a common reference time. The reference time for P_o (I^{131} and Sr^{89}) was D+0 (the time of the detonation). The reference times for A_m (I^{131}) and A_m (Sr^{89}) were D+5 and D+30 (5 and 30 days after the detonation) respectively.

The method of extrapolation for A_m was based on the averages of samples collected at a given time. For example, the average (time of collection) concentration of Sr^{89} in 20 bone ash samples collected on D+5 was 863 pc/g; and the average (time of collection) concentration in 20 samples collected at the same locations on D+ 30 was 2097 pc/g. In this case, extrapolation involved the multiplication of each D + 5 variate by $2097/863 = 2.433$.

The method of extrapolation for P_o was the same except that the correction factors for D + 5 variates were based on the average effective half-lives of I^{131} and Sr^{89} on plants from D + 5 to D + 15.

Some estimates of $T_p(I^{131})$ and $T_p(Sr^{89})$ were based on the arithmetic means ($\bar{x}P_t$) and the geometric means ($\bar{x}_g P_t$) of P_t as determined for 20 samples representing each time of collection. To study the frequency distributions of these variates, each estimate of $(T_p)_i$ was based on the individual values of $(P_t)_i$ representing two times of collection at each of the 20 stations.

The frequency distributions of $(T_p)_i$, P_o , and A_m for I^{131} and Sr^{89} and the frequency distributions of \log_{10} transforms representing the same variates were tested for normality (skewness and kurtosis) according to the procedure described by Snedecor⁽¹⁴⁾. (N. B. For the reader's convenience, the calculations involved in this procedure are illustrated in Appendix B.)

3.0 RESULTS

3.1 Radionuclide Concentrations in Plant Samples and Rabbit Tissues.

As shown in Table 1, the average concentrations of I^{131} and Sr^{89} in plant samples and of I^{131} in rabbit thyroids tended to decrease with increasing distance from ground zero and increasing time after the detonation. Average concentrations of Sr^{89} in rabbit bone ash were relatively low at D + 5 but reached maximum levels about D + 30 and then decreased to lower levels by D + 60.

The geometric means (\bar{x}_g) are consistently lower than the arithmetic means (\bar{x}); but usually, the matching groups of means are more or less proportional. In all but three cases (See the thyroid data for Penoyer on D + 25 and D + 30, the thyroid data for Currant on D + 15 and D + 20, and the bone ash data for Penoyer on D + 15 and D + 30.), the rank correlations between arithmetic and geometric means are perfect.

Table 1. Concentrations of I^{131} and Sr^{89} in plant samples (P_t) and in the thyroids or bone ash of rabbits (A_t) collected at different times (TOC=D+5, D+10, etc.) after the detonation from different areas in the Sedan fallout field.^{1/}

Radio - nuclides	Type of Sample	AREA:	GROOM		PENoyer		RAILROAD		CURRANT	
		TOC	\bar{x}	\bar{x}_g	\bar{x}	\bar{x}_g	\bar{x}	\bar{x}_g	\bar{x}	\bar{x}_g
I^{131}	P_t (pc/g)	D+ 5	11964	7741	1244	1021	713	698	501	477
		D+10	6671	4145	659	567	377	367	200	182
		D+15	3192	2243	412	341	211	204	121	73
		D+20	1224	664	226	159	119	113	56	47
		D+25	526	389	192	98	96	92	35	30
		D+30	273	191	103	80	48	42	26	24
	A_t (nc/g) thyroid)	D+ 5	466.6	331.0	257.2	200.9	105.9	75.4	26.2	23.2
		D+10	334.0	202.2	123.9	113.3	85.0	61.3	7.1	6.26
		D+15	138.9	86.6	74.6	55.7	60.9	47.6	5.9	3.52
		D+20	82.6	54.8	40.0	28.4	22.1	11.7	5.8	4.78
		D+25	61.2	41.4	28.7	18.4	28.8	15.3	1.6	1.56
		D+30	15.8	13.4	21.2	20.9	10.7	6.98	1.1	0.28
Sr^{89}	P_t (pc/g)	D+ 5	4079	2772	948	720	397	385	318	290
		D+15	2716	1685	470	394	269	262	183	168
		D+30	1584	1029	332	244	164	154	136	126
		D+60	788	502	283	204	127	90	55	53
	A_t (pc/g)	D+ 5	1459	814	1363	651	334	289	295	121
		D+15	3648	1009	2024	1461	620	313	323	273
		D+30	4999	2639	2283	935	783	598	427	286
		D+60	3581	2084	552	421	483	390	280	207

^{1/}Each value is the average of 5 samples: \bar{x} indicates the arithmetic means and \bar{x}_g indicates the geometric means of 5 samples from each area at each time of collection.

3.2 Fallout Particles and Radioactivity on Plant Foliage.

As shown in Fig. 2, autoradiographs of foliage indicated rather diffuse patterns of contamination. In most cases, the areas on X-ray films corresponding to individual leaves showed several to many dark spots imposed on a more or less uniformly gray, diffuse background. The areas on leaves corresponding to the dark spots on X-ray films were explored microscopically, but discoveries of measureable particles (i. e., particles $> 5 \mu$ in diameter) were infrequent in relation to the numbers of dark spots observed on the films. These observations suggest that most of the radioactivity on leaves was associated with particles (or aerosols) $< 5 \mu$ in diameter.

The results given in Table 2 show no consistent relationship between the observed number of radioactive particles per square centimeter of leaf surface (p/cm^2) and gamma activity ($c/m/cm^2$), concentrations of I^{131} or Sr^{89} in plant samples (Table 1), distance from ground zero, or time after the detonation. In fact, a comparison of data for Groom and Currant indicates entirely opposite trends. On D + 5, p/cm^2 was about 4 times higher in the Currant area while $c/m/cm^2$ was about 10 times higher in the Groom area. With increasing time after the detonation, $c/m/cm^2$ decreased in both areas; but p/cm^2 increased in the Groom area and decreased at Currant.

There are some indications of a nonlinear relationship between $c/m/cm^2$ (Table 2) and concentrations of I^{131} and Sr^{89} (Table 1) in the plant samples collected on D + 5; but there is no apparent correlation between p/cm^2 and either $c/m/cm^2$ and I^{131} or Sr^{89} concentrations (pc/g). The erratic changes in p/cm^2 and $c/m/cm^2$ in relation to time after the detonation could be

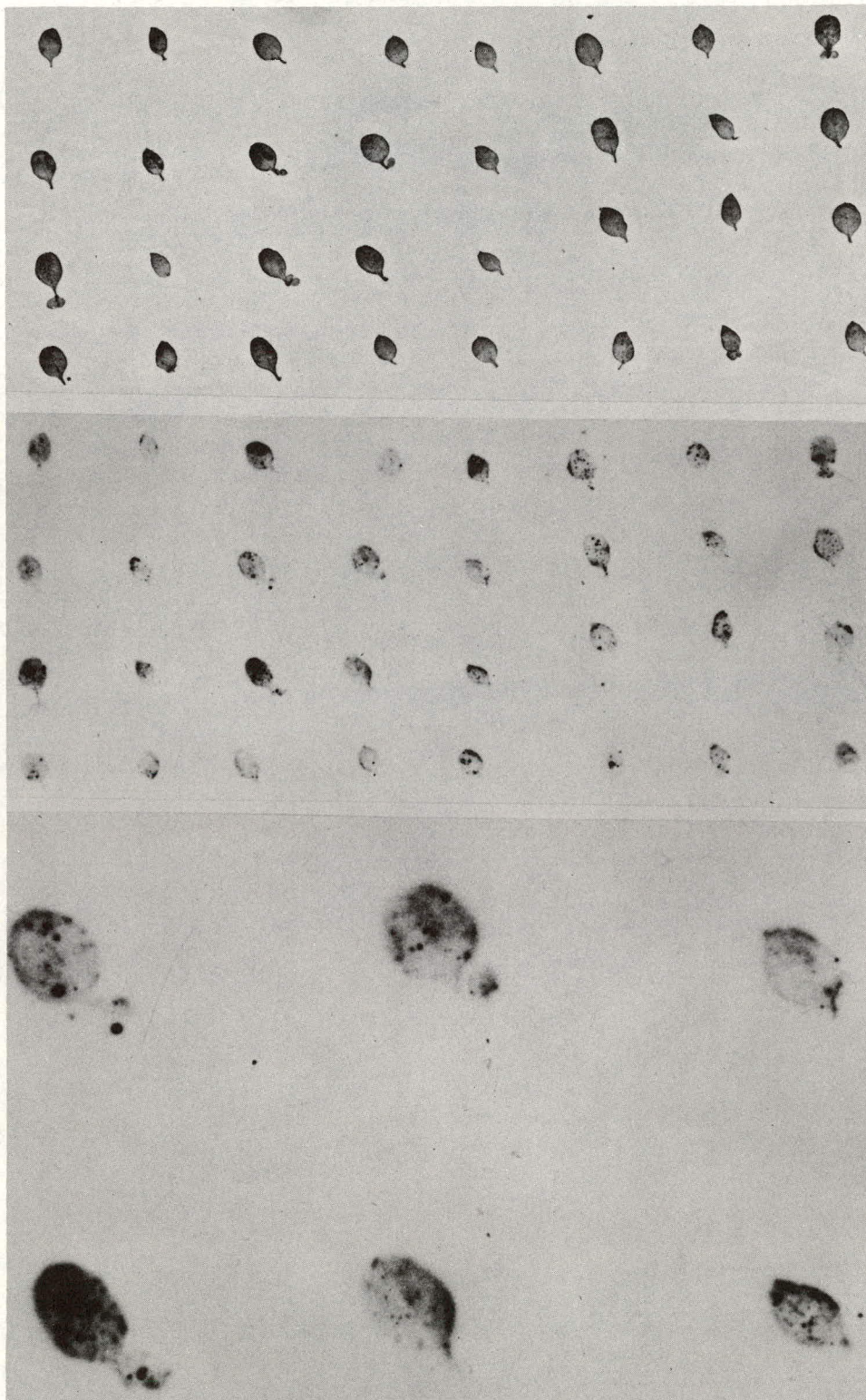


Figure 2. The autoradiographs of leaves mounted on transparent gummed paper showed a diffuse pattern of contamination with dark spots imposed on a more or less uniformly gray background.

Table 2. Number and size of radioactive particles (p/cm^2) and gross gamma activities ($c/m/cm^2$) on leaf samples from different parts of the Sedan fall-out field. Each value is the average of five samples.

Study Area	Measurement	D + 5	D+10	D+15	D+20	D+25	D+30
Groom	p/cm^2 , $<20\mu$	0.93	1.46	1.79	2.86	1.74	2.73
	p/cm^2 , 20-44 μ	0.68	0.81	0.73	1.03	2.06	1.95
	p/cm^2 , total ^{1/}	1.61	2.28	2.52	3.95	3.80	4.68
	$c/m/cm^2 \times 10^3$	517.6	88.4	54.5	69.2	35.5	25.8
Penoyer	p/cm^2 , $<20\mu$	0.58	0.55	0.45	0.74	0.87	1.08
	p/cm^2 , 20-44 μ	0.55	0.49	0.63	1.23	0.92	0.69
	p/cm^2 , total	1.13	1.07	1.08	1.97	1.81	1.92
	$c/m/cm^2 \times 10^3$	28.8	3.78	2.40	1.90	0.76	2.11
Railroad	p/cm^2 , $<20\mu$	2.60	1.21	0.28	1.39	0.52	1.39
	p/cm^2 , 20-44 μ	1.24	0.83	0.64	1.07	0.70	0.84
	p/cm^2 , total	3.86	2.04	0.94	2.47	1.22	2.26
	$c/m/cm^2 \times 10^3$	6.14	1.80	1.09	1.02	0.99	1.22
Currant	p/cm^2 , $<20\mu$	1.40	0.66	0.50	0.31	0.28	0.79
	p/cm^2 , 20-44 μ	3.25	1.03	1.23	2.01	0.82	0.71
	p/cm^2 , total	4.76	1.69	1.77	2.34	1.25	1.51
	$c/m/cm^2 \times 10^3$	5.77	0.72	0.39	0.23	0.29	0.19

^{1/} Total includes particles $> 44\mu$ in diameter.

interpreted as indications of fallout redistribution by wind action. The virtual absence of particles $> 44 \mu$ in diameter -- less than 2 per cent of all those measured -- seems to confirm the notion that virtually none of the radioactivity on leaves was associated with particles $> 44 \mu$ in diameter.

3.3 Retention Factors: Effective and Environmental Half-lives.

Estimates of the effective half-lives (T_p) and the environmental half-lives (T_E) of I^{131} and Sr^{89} on fallout-contaminated plants are given in Table 3. The estimates indicated by $T_p(\bar{x}P_t)$ and $T_p(\bar{x}_g P_t)$ are based on the means and geometric means of I^{131} and Sr^{89} concentrations (pc/g) in 20 samples representing each time of collection (D + 5, etc.) The estimates indicated by $(\bar{x}T_p)$ and $(\bar{x}_g T_p)$ are the means and geometric means of 20 different estimates of T_p each of which was based on the P_t values representing two times of collection at a given station.

The environmental half-life estimates (T_E) for I^{131} are mostly smaller than those for Sr^{89} , and this suggests that part of the I^{131} intercepted by plants may have been lost by some process such as vaporization which had no effect on the retention of Sr^{89} . The rate of this "other process" can be estimated by equation 3. For example, the T_E values indicated in Table 3 by $T_p(\bar{x}P_t)$ for I^{131} and Sr^{89} during the period from D + 5 to D + 30 are 13.1 and 27.4 days respectively. The effective rate of the other process (T_d) is given by $T_{dsi} = 27.4 \times 13.1 / 27.4 - 13.1 = 24.2$ days; and this suggests a significant difference in regard to the relative efficiency of I^{131} and Sr^{89} retention. Similar comparisons based on $T_p(\bar{x}_g P_t)$, $(\bar{x}T_p)$ and $(\bar{x}_g P_t)$ indicate $T_{dsi} = 31.3, 105.5,$ and 105.0 days respectively.

A reexamination of the $\log_{10} T_p$ data showed that the average environ-

Table 3. Estimates of effective half-lives (T_p) and environmental half-lives (T_E) based on the means (\bar{x}) and geometric means (\bar{x}_g) of I^{131} and Sr^{89} concentrations on plants (P_t) and on the individual variates ($(P_t)_i$) at different times of collection (D+5 to D+10, etc.)

Basis of Estimates ^{1/}	I^{131}					Sr^{89}		
	5-10	5-15	5-20	5-25	5-30	5-15	5-30	5-60
$T_p(\bar{x}P_t)$	5.76	5.35	4.76	4.89	4.98	15.2	17.8	25.2
T_E	20.3	15.0	11.7	12.5	13.1	22.5	27.4	52.4
$T_p(\bar{x}_g P_t)$	5.42	5.56	4.50	4.96	5.11	13.6	18.1	25.0
T_E	17.3	18.0	10.5	13.0	14.5	18.8	27.0	49.0
$(\bar{x}T_p)$	5.24	5.92	5.21	5.93	6.00	15.8	19.0	26.8
T_E	15.6	23.6	15.3	23.6	23.6	23.0	30.4	57.0
$(\bar{x}_g T_p)$	4.87	5.56	5.07	5.70	5.86	13.5	17.7	25.7
T_E	12.4	18.0	13.7	19.6	21.6	18.4	27.2	52.3

^{1/} For $n = 20$ and $i = 1$

$$(\bar{x}P_t) = \sum (P_t)_i / n$$

$$T_p(\bar{x}P_t) = 0.693 (t_2 - t_1) / \log_e \left[(\bar{x}P_{t_1}) / (\bar{x}P_{t_2}) \right]$$

$$(\bar{x}_g P_t) = \text{antilog} \sum \log_{10} (P_t)_i / n$$

$$T_p(\bar{x}_g P_t) = 0.693 (t_2 - t_1) / \log_e \left[(\bar{x}_g P_{t_1}) / (\bar{x}_g P_{t_2}) \right]$$

$$(T_p)_i = 0.693 (t_2 - t_1) / \log_e (P_{t_1} / P_{t_2})_i$$

$$(\bar{x}T_p) = \sum (T_p)_i / n$$

$$(\bar{x}_g T_p) = \text{antilog} \sum \log_{10} (T_p)_i / n$$

$$T_E = T_r \times T_p / T_r - T_p$$

$$T_r = 8.04 \text{ day } I-131, 50.5 \text{ day } Sr-89$$

mental half-lives of I^{131} and Sr^{89} from 5 to 30 days after the detonation at stations ($n = 7$) where the H + 24 gamma dose rates were ≥ 10 mr/hr were 14.5 and 29.0 days respectively ($T_{dsi} = 29$ days). Comparable estimates based on stations where the H + 24 dose rates were < 10 mr/hr ($n = 13$) indicated environmental half-lives of 25.6 and 29.6 days respectively for I^{131} and Sr^{89} ($T_{dsi} = 189.2$ days).

3.4 Interception Factors: Deposition on Soil vs. Interception by Plants.

Estimates of a_s (equation 4) were 95,870 and 23,400 $pc/ft^2/mr/hr$ for I^{131} and Sr^{89} , indicating a theoretical ratio of 4.097 for deposition on bare soil. As shown in Table 4, the average I^{131}/Sr^{89} ratio (independent of R_o) on plants in the Groom area was 4.374 while the comparable ratios for Penoyer, Railroad, and Currant were 2.210, 2.682, and 2.415 respectively.

Estimates of a_p (equations 5 and 6) ranged from 129 to 784 $pc/g/mr/hr$ for I^{131} and from 47 to 327 $pc/g/mr/hr$ for Sr^{89} . The average values of a_p for I^{131} and Sr^{89} interception by plants in the Groom area indicated a ratio of $(406.9 / 102.4 =) 3.97$, which is fairly close to the theoretical ratio indicated by a_s . Comparable ratios for Penoyer, Railroad, and Currant were 2.14, 2.63, and 2.17 respectively.

Since the averages of a_p estimates for Sr^{89} in Penoyer and Railroad were about the same as the average for Groom, the lower a_p values for I^{131} in Penoyer and Railroad suggest a deficiency of I^{131} relative to Sr^{89} . The higher a_p values in the Currant area may indicate an excess of both I^{131} and Sr^{89} relative to R_o , or they may be due to gross underestimates of R_o .

Since G and a_s were assumed to be constant, the $100 f_p$ (percentage interception as defined by equation 7) values in Table 4 vary only in relation to a_p . In the Groom area, where the species collected was

Table 4. Estimates of R_o (mr/hr) were based on aerial survey data (Fig. 1).

Estimates of P_o , a_p , and f_p were based on Eqs. 4-7. ^{1/}

Study Areas	R_o (mr/hr)	P_o			a_p		$100 f_p$	
		I^{131}	Sr^{89}	Ratio P_o 's	I^{131}	Sr^{89}	I^{131}	Sr^{89}
Groom	120.0	42193	8685	4.858	351.6	72.4	7.33	6.19
	80.0	36414	6487	5.613	455.2	81.1	9.50	6.93
	70.0	15158	3266	4.641	216.6	46.7	4.52	3.99
	25.0	17074	5575	3.063	683.0	223.0	14.2	19.0
	5.0	1641	444	3.696	323.2	88.8	6.85	7.59
\bar{x} :	60.0	22496	4891	4.374	406.9	102.4	8.49	8.75
Penoyer	40.0	5164	2878	1.795	129.1	71.9	2.69	6.14
	20.0	2865	1129	2.540	143.2	56.4	2.99	4.82
	8.0	1284	1279	1.004	160.5	159.9	3.35	13.7
	3.5	978	337	2.899	279.3	96.3	5.83	8.23
	3.0	1402	499	2.810	467.3	166.3	9.75	14.2
\bar{x} :	14.9	2339	1224	2.210	253.9	110.2	4.92	9.41
Railroad	10.0	1852	778	2.380	185.2	77.8	3.86	6.65
	7.0	1026	455	2.255	146.6	65.0	3.06	5.56
	6.0	1414	385	3.671	235.6	64.2	4.92	5.49
	3.5	1269	513	2.474	362.6	146.6	7.57	12.5
	3.0	1143	435	2.628	381.0	145.0	7.95	12.4
\bar{x} :	5.9	1341	513	2.682	262.2	99.7	5.47	8.52
Currant	2.0	1397	654	2.136	698.5	327.0	14.6	28.0
	1.8	912	385	2.369	506.7	213.9	10.6	18.3
	1.5	1083	535	2.024	722.0	356.7	15.0	30.5
	1.5	538	186	2.890	358.4	124.0	7.48	10.6
	1.0	748	295	2.658	748.0	295.0	16.4	25.2
\bar{x} :	1.56	943	411	2.415	613.9	283.3	12.8	22.5

^{1/} Estimates of P_o were based on concentrations of I^{131} and Sr^{89} in plant samples collected on D+5, $T_p(I^{131}) = 5.56$ days and $T_p(Sr^{89}) = 13.5$ days.

sagebrush (Artemisia tridentata), the average value of $100 f_p$ for Sr^{89} was 8.75 per cent. The comparable value for Penoyer and Railroad, where the species collected was shadscale (Atriplex confertifolia), was $9.41 + 8.52 / 2 = 8.96$ per cent. This comparison suggests only a slight difference between sagebrush and shadscale in regard to the interception of Sr^{89} . (One might assume that sagebrush is more efficient than shadscale in regard to I^{131} interception, but the a_p ratios for shadscale in Penoyer and Railroad was $(2.14 + 2.63 / 2 = 2.38)$ about the same as the ratio (2.17) for sagebrush in the Currant area.)

This line of reasoning indicates no large difference between sagebrush and shadscale in regard to the interception of I^{131} and Sr^{89} . It further suggests that the quantity $(f_p / G) = 0.0044 \text{ ft}^2/\text{g}$ could be treated as a constant for sagebrush and shadscale. According to this hypothesis, an alternative to the one defined by equations 4-7, variations in a_p would be attributed primarily to disparities between apparent and theoretical values of a_s , i. e., to the nonuniform distribution of I^{131} and Sr^{89} relative to estimates of R_o based on aerial survey data.

3.5 Frequency Distribution of Variates.

Figure 3 illustrates the frequency distributions of extrapolated values representing $P_o(Sr^{89})$. Histogram A shows the frequency distribution of the whole array ($n = 80$) based on estimates of the arithmetic mean and standard deviation. Histogram B shows the frequency distribution of the same array based on estimates of the mean and standard deviation of $\log_{10} P_o(Sr^{89})$. The shaded part of the histogram shows the frequency distribution of variates representing 7 stations where $R_o \geq 10 \text{ mr/hr}$ ($S \geq 10$) while the unshaded part shows the frequency distribution of variates

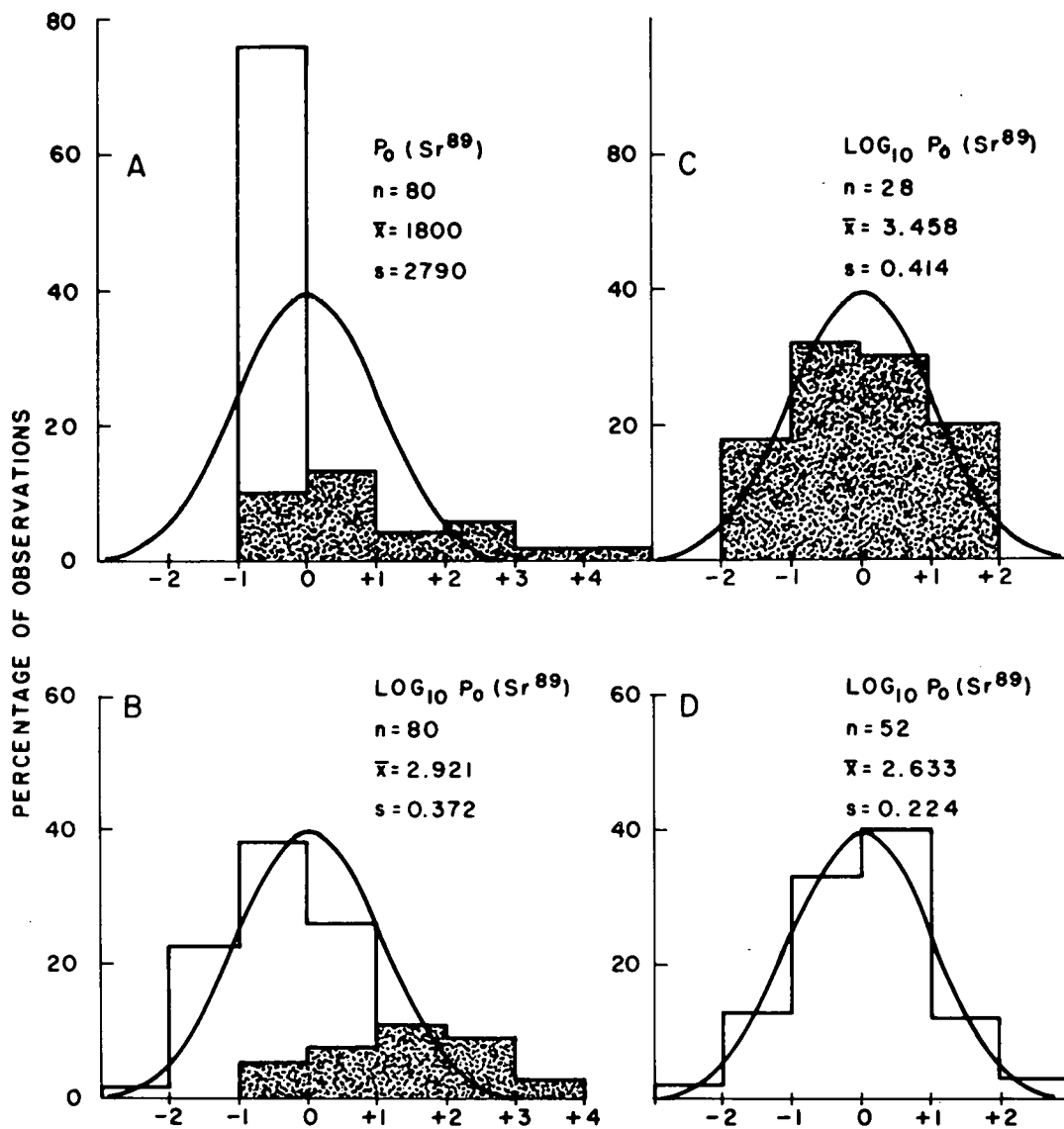


Fig. 3. Frequency distributions of $P_0(\text{Sr}^{89}) = \text{pc/g}$ of Sr^{89} on plants extrapolated to the time of the detonation where $n =$ number of samples, $\bar{x} =$ sample mean, and $s =$ sample standard deviation. Shaded areas indicate samples from $S \geq 10$; unshaded areas indicate samples from $S < 10$. The abscissa measurement is $= (X - \bar{x}) / s$. The areas under the normal curves are approximately equal to the areas of the histograms.

representing 13 stations where $R_0 < 10$ mr/hr ($S < 10$). Histograms C and D show the frequency distributions for $S \geq 10$ and $S < 10$ treated as different populations. Similar patterns were observed for extrapolated values representing P_0 (I^{131}), A_m (I^{131}), and A_m (Sr^{89}).

Statistics based on the frequency distributions of T_p estimates and extrapolated values of P_0 and A_m for I^{131} and Sr^{89} are given in Table 5. The statistics g_1 and g_2 are measures of skewness and kurtosis. Values of 0 for both g_1 and g_2 indicate perfect agreement between the observed and the expected (normal) frequency distribution. Positive values of g_1 indicate an excess of items below the mean while negative values indicate an excess of items above the mean. Positive values of g_2 indicate an excess of items near the mean and far from it while negative values indicate a flat-topped distribution curve due to a deficiency of items near the mean and far from it.

The frequency distributions of both T_p and $\log_{10} T_p$ were analyzed and compared. The results (Table 5) indicate normal frequency distributions for both T_p and $\log_{10} T_p$ variates representing $S \geq 10$ and $S < 10$; but when the variates representing these two groups are combined (ΣS), the results indicate significant or highly significant deviations from the normal frequency distributions. The large positive value of g_1 for T_p (I^{131}) ΣS indicates a highly significant excess of items below the arithmetic mean (5.67 days). Using $\log_{10} T_p$ (I^{131}) ΣS corrected the asymmetry and indicated a geometric mean of 5.40 days. (An earlier estimate (5) based on $(\bar{x}P_c)$ was 5.5 days.) The frequency distribution of T_p (Sr^{89}) ΣS showed negative skewness and positive kurtosis. Using $\log_{10} T_p$ (Sr^{89}) ΣS

Table 5. Statistics based on the frequency distributions of variates representing the effective half-lives (T_p), initial concentrations on plants (P_o), and maximum concentrations in rabbit tissues (A_m) of I^{131} and Sr^{89} in the Sedan fallout field.^{1/}

Variates	Stas.	n	\bar{x}	s	g_1	$t(g_1)$	g_2	$t(g_2)$	
I^{131}	T_p	$S \geq 10$	34	5.54	1.27	-0.776	-0.978	1.979	1.246
		$S < 10$	64	5.74	1.91	-0.633	-0.921	-1.311	-0.983
		ΣS	98	5.67	1.79	7.823	14.275**	0.023	0.042
$\log_{10} T_p$		$S \geq 10$	34	0.728	0.120	-0.528	-0.768	-0.110	-0.082
		$S < 10$	64	0.735	0.112	0.174	0.291	1.005	0.871
		ΣS	98	0.732	0.135	0.509	0.877	0.131	0.116
$\log_{10} P_o$		$S \geq 10$	42	4.009	0.522	0.623	0.869	-0.283	-0.202
		$S < 10$	78	3.124	0.334	0.504	0.703	1.408	1.006
$\log_{10} A_m$		$S \geq 10$	42	2.464	0.500	-0.791	-1.286	0.908	0.762
		$S < 10$	78	1.671	0.548	0.027	0.043	1.255	1.049
Sr^{89}	T_p	$S \geq 10$	21	21.9	2.85	1.051	1.466	0.820	0.587
		$S < 10$	37	19.6	1.28	-0.194	-0.244	-1.405	-0.885
		ΣS	58	18.8	7.9	-1.390	-2.390*	3.150	2.811**
$\log_{10} T_p$		$S \geq 10$	21	1.268	0.252	-0.511	-0.713	0.605	0.433
		$S < 10$	37	1.256	0.189	-0.024	-0.032	-1.699	-1.147
		ΣS	58	1.259	0.216	-0.980	-1.538	4.535	3.681**
$\log_{10} P_o$		$S \geq 10$	28	3.458	0.414	0.437	0.581	-0.592	-0.400
		$S < 10$	52	2.633	0.224	0.194	0.282	-1.933	-1.449
$\log_{10} A_m$		$S \geq 10$	28	3.521	0.455	-0.168	-0.212	-0.479	-0.301
		$S < 10$	52	2.575	0.433	0.141	0.213	-0.222	-0.174

^{1/} $S \geq 10$ and $S < 10$ indicate variates representing stations where $R_o \geq 10$

mr/hr ($n = 7$) and stations where $R_o < 10$ mr/hr ($n = 13$). ΣS indicates variates for all stations ($n = 20$) combined.

n = number of sample variates, \bar{x} = sample mean, s = sample standard deviation, g_1 = measure of skewness, g_2 = measure of kurtosis, $t(g_1)$ and $t(g_2)$ are estimates of significance

* Deviations from normal are significant at the 5% level of probability.

** Deviations from normal are significant at the 1% level of probability.

corrected the asymmetry but accentuated the kurtosis which is probably due to the nonuniform distribution of T_p (Sr^{89}) with respect to time after the detonation. The arithmetic mean of T_p (Sr^{89}), based on $n = 58$, was 18.8 days while the geometric mean was only 18.2 days. (An earlier estimate ⁽⁸⁾ based on $(\bar{x}P_t)$ was 18.0 days.)

The frequency distributions of $\log_{10} P_o$ and $\log_{10} A_m$ for I^{131} and Sr^{89} show no significant deviations from normal when the variates are grouped as representative of two populations, $S \geq 10$ and $S < 10$, as indicated in Fig. 3 and in Table 5. However, the \log_{10} means and standard deviations given in Table 5 are not necessarily the same as those of the real populations they represent because the method of extrapolation introduced an extraneous variable which increased the variance. For example, the data for $\log_{10} P_o$ (I^{131}) $S < 10$ (Table 5) indicates a mean and standard deviation of 3.124 ± 0.334 , and the individual variates ranged from 2.083 to 3.815. When the same group of original variates, $(P_t)_i$, were extrapolated to $(P_o)_i$ on the basis of individual half-life estimates $(T_p)_i$, the frequency distribution of variates $(\log_{10} P_o)_i$ was normal; but the simulated sample mean and standard deviation were 3.061 ± 0.147 , and the range of individual variates was from 2.743 to 3.443. This suggests that the method of extrapolation based on sample means produced simulated samples of P_o and A_m whose means and standard deviations are somewhat higher than the real populations they represent. However, there is no evidence that the method of extrapolation caused any significant change in the general form of the frequency distribution curves.

The means (\bar{x}) and geometric means (\bar{x}_g) of P_t and A_t for I^{131} and Sr^{89} representing $S \geq 10$ ($n = 7$) and $S < 10$ ($n = 13$) and ΣS ($n = 20$) are compared in Fig. 4. Both \bar{x} and \bar{x}_g are indicative of the large difference (approximately an order of magnitude) between $S \geq 10$ and $S < 10$. In most cases \bar{x} is larger than \bar{x}_g . For $S \geq 10$ and $S < 10$, the values of \bar{x} and \bar{x}_g are fairly close; but for ΣS , the differences between \bar{x} and \bar{x}_g are large. For $A_t(I^{131})$ and $A_t(Sr^{89})$ representing $S < 10$, the \bar{x} -values indicate time-specific variations which are considerably more erratic than those indicated by \bar{x}_g -values. This difference is probably attributable to a few exceptionally high (or low) variates which have a greater influence on \bar{x} than on \bar{x}_g .

It should be obvious, if the variates are lognormally distributed, that \bar{x}_g is a more useful parameter than \bar{x} . Table 6 was prepared to illustrate the kinds of errors resulting from the assumption of a normal distribution. The columns headed "S. M." are standard measures of the normal curve. Tau is given by $\tau = (X - \bar{x})/s$ where X is the magnitude of a given variate, \bar{x} is the sample mean, and s is the standard deviation of the sample mean. The values of X given in the body of Table 6 are based on $X = \bar{x} \pm \tau s$. Those indicated by N (normal) are based on the arithmetic means and standard deviations of P_o and A_m . Those indicated by L (lognormal) are the antilogarithms obtained from the means and standard deviations of $\log_{10} P_o$ and $\log_{10} A_m$. The column headed "C. P." indicates the cumulative percentage of variates expected to be less than or equal to the magnitudes of X indicated in columns N or L. Comparing columns N and L for the several groups of variates shows that

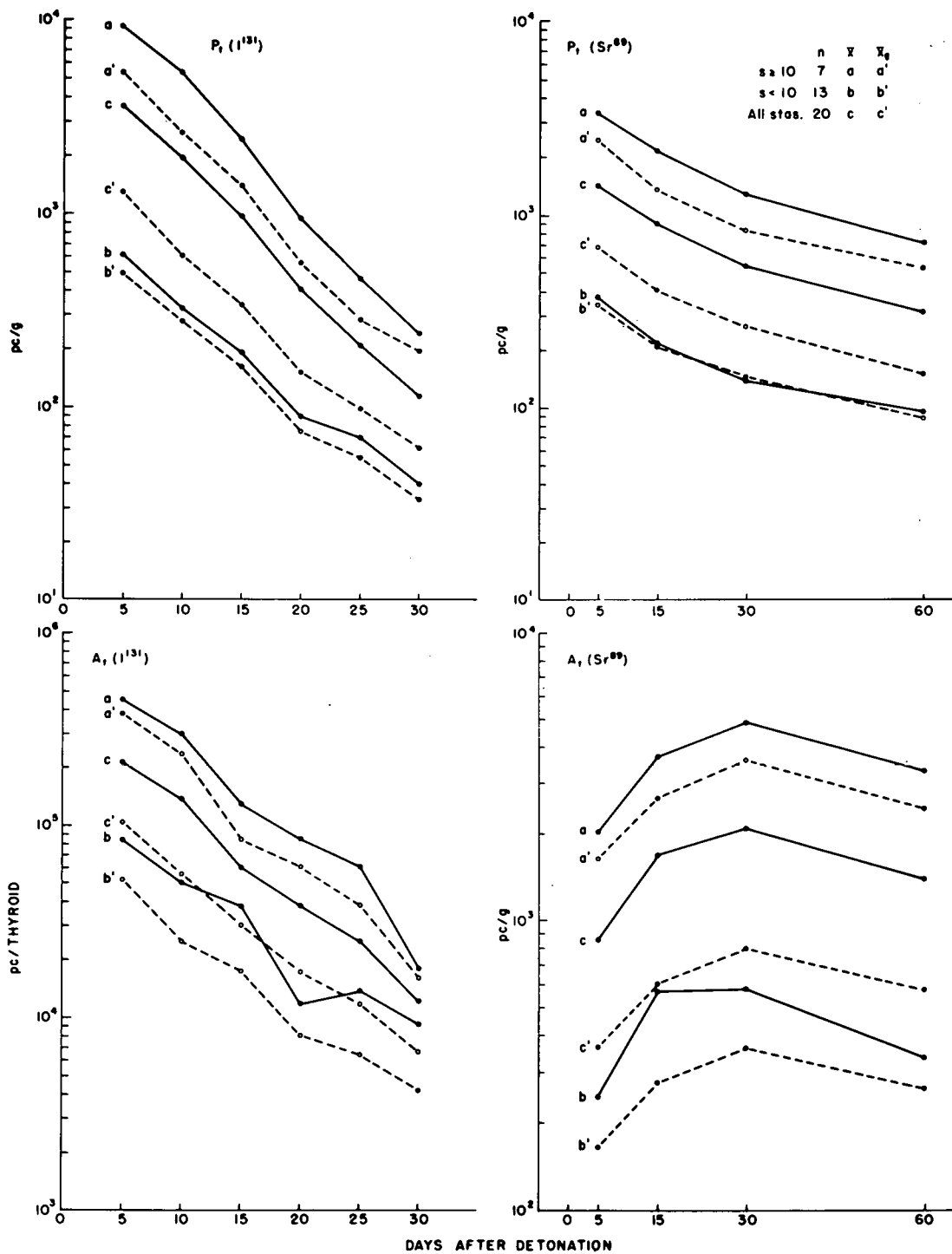


Fig. 4. Comparison of means (\bar{x}) and geometric means (\bar{x}_g) of $P_t(I^{131})$, $A_t(I^{131})$, $P_t(Sr^{89})$, and $A_t(Sr^{89})$ for $S \geq 10$ ($n = 7$), $S < 10$ ($n = 13$) and ΣS ($n = 20$).

Table 6. Estimated frequency distributions of variates representing the initial concentrations on plants (P_o) and the maximum concentrations in rabbit tissues (A_m) of I^{131} and Sr^{89} in the Sedan fallout field.^{1/}

S. M.		S _≥ 10		S _{<} 10		S _≥ 10		S _{<} 10	
γ	C. P.	N	L	N	L	N	L	N	L
		$P_o (I^{131})$				$A_m (I^{131})$			
-1.96	2.5	-12886	969	-577	294	-169	30	-144	3.95
-1.65	5.0	- 8062	1383	-211	373	- 75	44	-105	5.84
-1.29	10.0	- 2460	2166	213	493	34	60	- 60	9.20
-0.85	20.0	4386	3677	732	691	149	109	5	16.0
-0.53	30.0	9365	5525	1109	884	264	158	35	24.0
0.00	50.0	17612	10205	1734	1330	425	291	101	46.8
0.53	70.0	25859	19290	2359	1999	586	536	157	91.4
0.85	80.0	30838	28330	2736	2557	682	775	207	135.9
1.29	90.0	37684	48060	3255	3588	816	1286	262	238.5
1.65	95.0	43286	74070	3679	4735	925	1946	307	375.7
1.96	97.5	48110	107730	4045	6011	1019	2781	346	555.5
		$P_o (Sr^{89})$				$A_m (Sr^{89})$			
-1.96	2.5	- 2904	443	22	156	-2356	425	-750	48.7
-1.65	5.0	- 1774	595	59	183	-1213	588	-536	67.2
-1.29	10.0	462	839	153	221	115	858	-287	97.9
-0.85	20.0	1142	1276	267	277	1738	1362	17	155
-0.53	30.0	2308	1732	350	327	2919	1903	238	216
0.00	50.0	4240	2870	488	429	4874	3317	604	376
0.53	70.0	6172	4756	626	564	6829	5780	970	653
0.85	80.0	7338	6455	709	666	8009	8082	1191	911
1.29	90.0	8942	9820	823	835	9633	12815	1495	1441
1.65	95.0	10254	13840	917	1005	10961	18690	1744	2098
1.96	97.5	11384	18605	998	1180	12104	25864	1958	2899

^{1/} S. M. : standard measures of the normal curve, $\gamma = (X - \bar{x}) / s$;
 C.P. = cumulative percentage of variates $\geq X$ as given in the body of the table. Columns headed by N are based on the assumption of normal distributions and $X = \bar{x} \pm \gamma s$; Columns headed by L are based on the assumption of lognormal distributions and $X = \text{antilog } \bar{x}(\log_{10}) \pm \gamma s(\log_{10})$. $S \geq 10$ and $S < 10$ indicate variates representing stations where $R_o \geq 10$ or $R_o < 10$ mr/hr. Additional explanations are given in the text.

the erroneous assumption of normal distributions may result in (1) overestimates of the mean and values near the mean, (2) underestimates of values far from the mean, and (3) negative values, which are untenable, far below the mean.

4.0 DISCUSSION

4.1 Radionuclide Concentrations in Plant Samples and Rabbit Tissues.

The results given in Table 1 showed that the maximum concentrations of I^{131} and Sr^{89} in plant samples and rabbit tissues decreased with increasing distance from ground zero and decreasing gamma dose rates at H + 24. In this respect, the four study areas -- Groom, Penoyer, Railroad, and Currant -- could be ranked as follows: $G \gg P \gg R > C$. Similar results were indicated (Appendix A) for Sr^{90} and Cs^{137} , but the postshot concentrations of these radionuclides were not significantly higher than the preshot concentrations at more than half of the 20 sampling stations.

The time-specific relationships between I^{131} and Sr^{89} concentrations on plants and in rabbit thyroids and bone ash were illustrated in Fig. 4. The formulation of deterministic and stochastic models to represent these relationships and the potential uses of such models in predicting radionuclide levels and tissue doses resulting from a single fallout event were discussed in earlier papers (4-9).

4.2 Fallout Particles and Radioactivity on Plant Foliage.

While the results given in Table 2 showed no consistent relationship between the number of particles 5 to 44 μ in diameter (p/cm^2) and gross gamma activity ($c/m/cm^2$) per unit area of leaf surface, the ranking of study areas on the basis of $c/m/cm^2$ was the same as the ranking based

on radionuclide concentrations, i. e., $G \gg P \gg R > C$. In all study areas, the gamma activities ($c/m/cm^2$) and the radionuclide concentrations (pc/g) decreased with increasing time after the detonation, but the number of particles per unit area (p/cm^2) decreased in some areas and increased in others.

These results and the general appearance of autoradiographs suggested that most of the radioactivity deposited on plants in all four study areas was due to particles smaller than the optical resolution of the microscope used to measure them, i. e., $< 5 \mu$ in diameter. Since particles $> 44 \mu$ in diameter accounted for < 2 per cent of all those measured, we may assume that virtually all the activity deposited on plants was associated with particles $< 44 \mu$ in diameter. These results are similar to those reported earlier by Romney et al. ⁽²⁾

The apparently erratic changes in p/cm^2 and $c/m/cm^2$ (Table 2) with increasing time after the detonation may be the results of fallout redistribution by wind. For example, the increasing number of particles per unit area of leaf surface in the Groom study area, which is northeast of ground zero, may have been due to the continuing postshot deflation by southwesterly winds of materials initially deposited close to ground zero. While the effects of redistribution on fallout retention by plants are not precisely known, it has generally been assumed ⁽¹⁾ that mechanical disturbances by wind (or rain) cause radionuclide losses in excess of radioactive decay.

4.3 Retention Factors: Effective & Environmental Half-lives.

The results given in Table 3 showed that the effective half-lives of I^{131} and Sr^{89} on fallout-contaminated plants (approximately 5.5 and 18 days

respectively) were significantly shorter than their radioactive half-lives (8.04 and 50.5 days respectively). The effective half-life of I^{131} on plants was more or less uniform with respect to time (5 to 30 days) after the detonation, but the effective half-life of Sr^{89} apparently increased with increasing time (5 to 60 days) after the detonation. (N. B. Since the rate of loss was not strictly exponential, the use of "half-life" in reference to Sr^{89} retention by plants is technically inaccurate; but in this case, the estimated rate in half-life terms is a useful approximation of the true rate.)

Estimates of the environmental half-life (T_E) of I^{131} were mostly smaller than estimates of the environmental half-life of Sr^{89} . This may have been due to the loss of I^{131} by some process, probably vaporization, which had no effect on the retention of Sr^{89} . Comparisons of effective (T_p) and environmental (T_E) half-life estimates for I^{131} and Sr^{89} representing $S \geq 10$ and $S < 10$ suggested that the probability of I^{131} loss by vaporization was greatest in areas relatively close to ground zero.

The differences between effective and radioactive half-lives of radionuclides on plants lower the availability of radionuclides for ingestion by herbivores and hence for transfer to higher trophic levels. In the case of long-lived radionuclides, such as Sr^{90} and Cs^{137} , there may be several orders of magnitude difference between the radioactive and effective half-lives. In studies of food chain kinetics and in comparison of plant vs. soil contributions to tissue burdens failure to consider this factor could lead to serious errors.

4.4 Interception Factors: Deposition on Soil vs. Interception by Plants.

No attempt was made in this study to consider all the factors which

which could influence the interception and retention of fallout radionuclides by plants. Instead, we proposed a fairly simple hypothesis (equations 4-7) to explain the basic interrelations of H + 24 gamma dose rates, hypothetical concentrations (pc/ft²/mr/hr) of I¹³¹ and Sr⁸⁹ on soil, and observed concentrations (pc/g/mr/hr) on plants. (N. B. An earlier report by Miller⁽¹⁵⁾ and a recent review paper by Russell⁽¹⁶⁾ present more detailed analyses of the problem.)

The results given in Table 4 suggested (1) an apparent deficiency of I¹³¹ deposition relative to Sr⁸⁹ deposition in all study areas except Groom, the area closest to ground zero, and (2) an apparent excess of both I¹³¹ and Sr⁸⁹ deposition relative to gamma dose rates (R_0) in the Currant study area, the one farthest from ground zero. Since the data provided no firm evidence of a significant difference between sagebrush (collected in the Groom and Currant study areas) and shadscale (collected in Penoyer and Railroad Valleys) in respect to their interception of I¹³¹ and Sr⁸⁹, I believe that most of the variation observed in relation to initial concentrations on plants could probably be attributed to the nonuniform distribution of these radionuclides in relation to R_0 , i. e., to fractionation and/or to errors in estimating R_0 from aerial survey data.

The assumption of I¹³¹ loss by vaporization before fallout deposition could explain the apparent deficiency of I¹³¹ deposition in study areas more distant from ground zero than Groom. The assumption of I¹³¹ loss by vaporization after fallout deposition could explain the shorter environmental half-life of I¹³¹ in areas relatively close to ground zero. The apparent excess of both I¹³¹ and Sr⁸⁹ may have been due to a combination of meteorological and orographic conditions similar to those involved in

the development of "hot-spots" at even greater distances from ground zeros.

The data collected from the Currant study area may also indicate a marked tendency for the percentage interception of fallout by plants to increase as total fallout deposition, indicated by R_0 , decreases. If this tendency is real and if it extends beyond the limits of the present study, one could expect to find significant concentrations of I^{131} and Sr^{89} on plants in areas where increased gamma dose rates due to fallout are barely distinguishable from background.

4.5 Lognormal vs. Normal Frequency Distributions.

The results given in Fig. 3 and Table 5 provided evidence that variates representing the initial concentrations (P_0) of I^{131} and Sr^{89} on fallout-contaminated plants and subsequent maximum concentrations (A_m) of I^{131} in rabbit thyroids and of Sr^{89} in rabbit bone ash are lognormally distributed. Figure 3, and similar comparisons not illustrated in this paper, showed that P_0 and A_m variates representing $S \geq 10$ and $S < 10$ were apparently drawn from different populations. The results given in Table 5 suggested that the same assumption should be made in regard to effective half-life estimates, but both T_p and $\log_{10} T_p$ could then be treated as normally distributed variates.

The lognormal frequency distributions of variates representing radionuclide concentrations in plant samples and rabbit tissues are probably related to the manner in which fallout is initially distributed in the fallout field.

As shown in Fig. 1, the distance between H + 24 gamma dose rate contours tends to increase with increasing distance from ground zero. Using a planimeter to estimate the areas between contour intervals gave

the following results: 50 mi² between 1000 and 100 mr/hr, 450 mi² between 100 and 10 mr/hr, and 4500 mi² between 10 and 1 mr/hr. (N. B. These data indicate radioactivity approximately equivalent to one kiloton of fission products spread over an area of 5000 mi².) While these are rough estimates, they seem to indicate that the log₁₀ of H + 24 gamma dose rate contours are inversely proportional to the log₁₀ of areas (mi²) inclosed by the contours. In other words, 10-fold increases in the area of the fallout field are accompanied by 10-fold decreases in the H + 24 gamma dose rates at the perimeters of the areas.

Figure 4 showed that the arithmetic means (\bar{x}) of P_t and A_t were higher than the geometric means (\bar{x}_g) of the same samples, but the correlation of \bar{x} and \bar{x}_g was good enough to warrant the use of either set in estimating rates of change or relative differences in magnitude.

The results given in Table 6 showed that the assumption of normal frequency distributions of variates representing P_o and A_m resulted in overestimates of the means and values near the means and underestimates (even negative numbers) of values far from the means.

These observations suggest that estimates of population exposures based on arithmetic means (e. g., on the average concentrations of radionuclides in milk or other human foods) may be somewhat pessimistic. On the other hand, the assumption that critical variates may be lognormally distributed implies a relatively higher frequency of individuals exposed to radionuclide levels 2 or 3 times the average for the population. In view of these discrepancies, it would be a desirable practice -- before drawing inferences or basing conclusions on samples of radionuclide concentrations in environmental media, foods, or human tissues -- to determine whether

the variates are normally or lognormally distributed. The procedure described by Snedecor ⁽¹⁴⁾ is relatively simple, and it could quite conceivably lead to a more realistic evaluation of biological hazards related to environmental contamination by fallout.

REFERENCES CITED

1. W. E. Martin, Losses of Sr^{90} , Sr^{89} , and I^{131} from fallout-contaminated plants, *Radiation Botany*, 4:275-284 (1964).
2. E. M. Romney, R. G. Lindberg, H. A. Hawthorne, B. G. Bystrom, and K. H. Larson, Contamination of plant foliage with radioactive fallout, *Ecology*, 44: 343-349 (1963).
3. National Academy of Science, The behavior of radioactive fallout in soils and plants, National Research Council, Publ. 1092: 1-32 (1963).
4. F. B. Turner, The uptake of fallout radioisotopes by mammals and a stochastic simulation of the process, in U. S. AEC Report TID-7701 (1965).
5. F. B. Turner and W. E. Martin, Food-chain relationships of radioiodine following two nuclear tests in Nevada, U. S. AEC Report PNE-236P (1963).
6. F. B. Turner and W. E. Martin, Food-chain relationships of I^{131} following the Sedan test of July 6, 1962, U. S. AEC Report PNE-236F (1964).
7. W. E. Martin, Early food-chain kinetics of radionuclides following close-in fallout from a single nuclear detonation, in: U. S. AEC Report TID-7701 (1965).
8. W. E. Martin and F. B. Turner, Food-chain relationships of radiostrontium in the Sedan fallout field, U. S. AEC Report PNE-237F (1965).
9. M. D. Nordyke, Cratering experience with chemical and nuclear explosives, in: U. S. AEC Report TID-7695 (1964).
10. R. G. Guillou, Aerial radiometric survey, Project Sedan, U. S. AEC Report PNE-225P, Part 2 (1963).
11. Samuel Glasstone (ed.), The Effects of Nuclear Weapons, U. S. Government Printing Office, Washington, D. C. (1962).

12. S. Katcoff, Fission-product yields from neutron-induced fission, *Nucleonics*, 18(11): 201-208 (1960).
13. G. Higgins, Calculation of radiation fields from fallout. U. S. AEC Report UCID-4539 (1963).
14. G. W. Snedecor, Statistical Methods, 5th ed., Iowa State University Press, Ames, Iowa (1962).
15. C. F. Miller, Fallout and Radiological Countermeasures, 2 vols., Stanford Research Institute, Menlo Park, Calif. (1963).
16. R. S. Russell, Interception and retention of airborne material on plants, *Health Physics*, 11(12): in press (1965).

Appendix A. Concentrations (pc/g) of Sr⁹⁰ and Cs¹³⁷ in plant samples

collected before (Bkg) and at various times after (D + 5 etc.) the detonation from 20 representative locations in the Sedan fallout field.

Area & Sta. *	Strontium - 90					Cesium - 137				
	Bkg	D+5	D+15	D+30	D+60	Bkg	D+5	D+15	D+30	D+60
G- 3	3.0	73.2	59.9	48.5	28.9	4.8	226.0	130.5	67.8	45.6
G- 6	1.4	50.2	23.5	15.5	11.2	3.2	200.0	77.0	14.0	9.1
G- 7	9.8	48.0	22.8	22.6	19.4	19.8	83.1	59.4	42.3	22.5
G- 8	1.0	28.1	12.9	8.7	5.8	1.4	73.8	30.2	15.2	9.7
P-16	NS	7.3	5.0	12.2	5.8	NS	47.7	22.2	13.0	10.8
P-17	NS	17.9	8.9	9.5	12.5	NS	59.5	24.8	14.6	29.8
Avg.	3.8	37.4	22.2	19.5	13.9	7.3	115.0	57.4	27.8	21.2
R-15	1.5	4.9	3.3	3.0	3.0	1.9	16.6	7.6	5.2	5.2
P-10	NS	3.9	NS	2.2	4.6	NS	18.0	10.4	5.0	7.2
R-14	NS	3.6	3.0	3.0	3.0	NS	10.6	4.6	1.9	3.0
G- 5	1.8	4.7	3.6	2.5	2.6	2.0	12.2	5.8	2.2	NS
R-12	3.3	2.7	3.2	2.6	3.3	5.5	8.4	4.5	3.1	3.3
P- 8	1.4	3.3	3.2	3.0	3.1	1.0	10.0	8.7	9.5	3.4
P- 9	NS	3.7	2.8	3.3	3.1	NS	19.3	6.3	5.2	5.4
R- 5	NS	4.1	4.2	5.0	3.8	NS	12.8	5.0	7.3	2.3
R-10	1.3	4.0	3.4	3.4	4.2	1.5	8.4	7.2	4.7	4.9
C- 1	1.0	5.6	7.2	5.3	3.7	1.0	21.0	10.5	8.2	3.8
C- 2	4.2	5.4	5.4	4.9	4.1	4.9	11.3	8.7	4.7	4.1
C- 3	8.8	5.0	4.0	4.0	2.6	4.7	12.0	6.5	4.1	2.6
C- 4	6.7	4.3	4.0	2.8	2.4	3.9	7.7	NS	3.3	3.3
C- 5	4.0	4.0	4.7	4.0	4.2	3.7	8.9	4.6	3.3	3.4
Avg.	3.4	4.2	4.0	3.5	3.4	3.0	12.7	6.9	4.8	4.0

* G, P, R, and C refer to the Groom, Penoyer, Railroad, and Currant study areas.

(See Fig. 1). NS = no sample, or sample lost.

Appendix B. Test of normality based on estimates of the effective half-life (T_p) of I^{131} on plants at locations ($S < 10$) where the H + 24 gamma dose rate was < 10 mr/hr. (See Table 5).

Class	Intervals	f	X	(fX)	(fX) ²	(fX) ³	(fX) ⁴
2.01	- 3.00	4	-4	-16	256	-4,096	65,536
3.01	- 4.00	8	-3	-24	576	-13,824	331,776
4.01	- 5.00	14	-2	-28	784	-21,952	614,656
5.01	- 6.00	15	-1	-15	225	-3,375	50,625
6.01	- 7.00	8	0	0	0	0	0
7.01	- 8.00	8	1	8	64	512	4,096
8.01	- 9.00	4	2	8	64	512	4,096
9.01	- 10.00	1	3	3	9	27	81
10.01	- 11.00	1	4	4	16	64	256
11.01	- 12.00	1	5	5	25	125	625
Σ :		64	1	-55	2,019	-42,007	1,071,747

f = frequency of variates in each class

Σf = total number of variates in sample

n = number of classes = 10

X = assigned code numbers

$$s_1 = \Sigma (fX) = -55$$

$$s_2 = \Sigma (fX)^2 = 2,019$$

$$s_3 = \Sigma (fX)^3 = -42,007$$

$$s_4 = \Sigma (fX)^4 = 1,071,747$$

$$S_2 = s_2 - (s_1^2/n) = 1,717$$

$$S_3 = s_3 - (3s_1s_2/n) + 2(s_1^3/n^2) = -12,021$$

$$S_4 = s_4 - (4s_1s_3/n) + (6s_1^2s_2/n^2) - (3s_1^4/n^3) = 486,589$$

$$K_2 = S_2 / (n-1) = 190.8$$

$$K_3 = nS_3 / (n-1)(n-2) = -1,669.6$$

$$K_4 = (nS_4(n+1) - 3(n-1)S_2^2) / (n-1)(n-2)(n-3) = -51,641$$

$$g_1 = K_3 / K_2 \sqrt{K_2} = \underline{-0.633}$$

$$g_2 = K_4 / K_2^2 = \underline{-1.311}$$

$$(s_{g_1})^2 = 6n(n-1) / (n-2)(n+1)(n+3) = 0.472$$

$$s_{g_1} = \underline{0.687}$$

$$(s_{g_2})^2 = 24n(n-1)^2 / (n-3)(n-2)(n+3)(n+5) = 1.780$$

$$s_{g_2} = \underline{1.334}$$

$$t_{g_1} = g_1 / s_{g_1} = -0.633 / 0.687 = \underline{-0.921}$$

$$t_{g_2} = g_2 / s_{g_2} = -1.311 / 1.334 = \underline{-0.983}$$

After Snedecor (14)

TECHNICAL REPORTS SCHEDULED FOR ISSUANCE
BY AGENCIES PARTICIPATING IN PROJECT SEDAN

AEC REPORTS

<u>AGENCY</u>	<u>PNE NO.</u>	<u>SUBJECT OR TITLE</u>
USPHS	200F	Off-Site Radiation Safety
USWB	201F	Analysis of Weather and Surface Radiation Data
SC	202F	Long Range Blast Propagation
REECO	203F	On-Site Rad-Safe
AEC/USBM	204F	Structural Survey of Private Mining Operations
FAA	205F	Airspace Closure
SC	211F	Close-In Air Blast From a Nuclear Event in NTS Desert Alluvium
LRL-N	212P	Scientific Photo
LRL	214P	Fallout Studies
LRL	215F	Structure Response
LRL	216P	Crater Measurements
Boeing	217P	Ejecta Studies
LRL	218P	Radioactive Pellets
USGS	219F	Hydrologic Effects, Distance Coefficients
USGS	221P	Infiltration Rates Pre and Post Shot
UCLA	224P	Influences of a Cratering Device on Close-In Populations of Lizards
UCLA	225P Pt. I and II	Fallout Characteristics

TECHNICAL REPORTS SCHEDULED FOR ISSUANCE
BY AGENCIES PARTICIPATING IN PROJECT SEDAN

<u>AGENCY</u>	<u>PNE NO.</u>	<u>SUBJECT OR TITLE</u>
BYU	226P	Close-In Effects of a Subsurface Nuclear Detonation on Small Mammals and Selected Invertebrates
UCLA	228P	Ecological Effects
LRL	231F	Rad-Chem Analysis
LRL	232P	Yield Measurements
EGG	233P	Timing and Firing
WES	234P	Stability of Cratered Slopes
LRL	235F	Seismic Velocity Studies

DOD REPORTS

<u>AGENCY</u>	<u>PNE NO.</u>	<u>SUBJECT OR TITLE</u>
USC-GS	213P	"Seismic Effects From a High Yield Nuclear Cratering Experiment in Desert Alluvium"
NRDL	229P	"Some Radiochemical and Physical Measurements of Debris from an Underground Nuclear Explosion"
NRDL	230P	Naval Aerial Photographic Analysis

ABBREVIATIONS FOR TECHNICAL AGENCIES

STL	Space Technology Laboratories, Inc., Redondo Beach, Calif.
SC	Sandia Corporation, Sandia Base, Albuquerque, New Mexico
USC&GS	U. S. Coast and Geodetic Survey, San Francisco, California
LRL	Lawrence Radiation Laboratory, Livermore, California
LRL-N	Lawrence Radiation Laboratory, Mercury, Nevada
Boeing	The Boeing Company, Aero-Space Division, Seattle 24, Washington
USGS	Geological Survey, Denver, Colorado, Menlo Park, Calif., and Vicksburg, Mississippi
WES	USA Corps of Engineers, Waterways Experiment Station, Jackson, Mississippi
EGG	Edgerton, Germeshausen, and Grier, Inc., Las Vegas, Nevada, Santa Barbara, Calif., and Boston, Massachusetts
BYU	Brigham Young University, Provo, Utah
UCLA	UCLA School of Medicine, Dept. of Biophysics and Nuclear Medicine, Los Angeles, Calif.
NRDL	Naval Radiological Defense Laboratory, Hunters Point, Calif.
USPHS	U. S. Public Health Service, Las Vegas, Nevada
USWB	U. S. Weather Bureau, Las Vegas, Nevada
USBM	U. S. Bureau of Mines, Washington, D. C.
FAA	Federal Aviation Agency, Salt Lake City, Utah
REECO	Reynolds Electrical and Engineering Co., Las Vegas, Nevada

SUPPLEMENTARY DOD DISTRIBUTION FOR PROJECT SEDAN

<u>PNE NO.</u>	<u>DIST. CAT.</u>	<u>PNE NO.</u>	<u>DIST. CAT.</u>	<u>PNE NO.</u>	<u>DIST. CAT.</u>
200	26, 28	214	26	226	42
201	2, 26	215	32	228	42
202	12	216	14	229	26, 22
203	28	217	14	230	100
204	32	218	12, 14	231	22
205	2	219	14	232	4
211	12	221	14	233	2
212	92, 100	224	42	234	14
213	12, 14	225	26	235	14

In addition, one copy of reports 201, 202, 203, 211, 214, 215, 216, 217, 218, 221, 225, 229, 230, 232, 234, and 235 to each of the following:

The Rand Corp.
1700 Main St.,
Santa Monica, California

Attn: Mr. H. Brode

U. of Illinois,
Civil Engineering Hall
Urbana, Illinois

Attn: Dr. N. Newmark

Stanford Research Institute
Menlo Park, California

Attn: Dr. Vaile

E. H. Plesset Associates
1281 Westwood Blvd.,
Los Angeles 24, California

Attn: Mr. M. Peter

Mitre Corp.
Bedford, Massachusetts

General American Transportation Corp.
Mechanics Research Div.
7501 N. Natchez Ave.,
Niles 48, Illinois

Attn: Mr. T. Morrison; Dr. Schiffman

Dr. Whitman
Massachusetts Institute of Technology
Cambridge, Massachusetts

